Relationship of Thematic Mapper Simulator Data to Leaf Area Index of Temperate Coniferous Forests

DAVID L. PETERSON

NASA / Ames Research Center, Moffett Field, California 94035

MICHAEL A. SPANNER

TGS Technology, Inc., NASA / Ames Research Center, Moffett Field, California 94035

STEVEN W. RUNNING

School of Forestry, University of Montana, Missoula, Montana 59812

and

KURT B. TEUBER

Southern Forest Experimental Station, USDA Forest Service, Starkville, Mississippi, 39759

Regional relationships between remote sensing data and the leaf area index (LAI) of coniferous forests were analyzed using data acquired by an Airborne Thematic Mapper (ATM). Eighteen coniferous forest stands with a range of projected leaf area index of 0.6–16.1 were sampled from an environmental gradient in moisture and temperature across west-central Oregon. Spectral radiance measurements to account for atmospheric effects were acquired above the canopies from a radiometer mounted on a helicopter. A strong positive relationship was observed between the LAI of closed canopy forest stands and the ratio of near-infrared (0.76–0.90 μm) and red (0.63–0.69 μm) spectral bands. A linear regression based on LAI explained 83% of the variation in the ratio of the atmospherically corrected bands. A log-linear equation fit the asymptotic characteristic of the relationship better, explaining 91% of the variance. The positive relationship is explained by a strong asymptotic inverse relationship between LAI and red radiation and a relatively flat response between LAI and near infrared radiation.

Introduction

The development of plant canopies is related to underlying ecological and physiological processes. The plant canopy is important as the locus of exchange of energy, water, momentum, nutrients, and biogenic compounds. Grier and Running (1977) demonstrated that decreasing site water balance limited leaf development for coniferous forest stands along a temperature-moisture gradient in Oregon. For a similar gradient, Gholz (1982) reported a direct linear relationship between the LAI of conifer forests and above ground net primary production. In Running's (1984) model of evapotranspiration and photosynthesis in conifer ecosystems, LAI is used to calculate minimum light levels within the canopy regulating stomatal opening, precipitation interception, and absorption of photosynthetically active radiation.

The structural, morphological, phenological, and biochemical properties of forest canopies have been related to functional processes; yet measurement of these properties over the spatial and temporal

52 Vanderbilt Ave., New York, NY 10017 0034-4257/87/$3.50

scales of large regions remains particularly difficult. If remote sensing techniques can be used to reliably measure key structural variables like leaf area index, and LAI can be used as an index to functional processes like net primary productivity, then the uniform, synoptic, large scale capabilities of remote sensing from satellites could make substantial contributions to regional and global ecological studies (Rambler, 1983; Wittwer, 1983).

The research reported here describes measurements of the LAI of temperate coniferous forests across a regional gradient, and the relationship of LAI to variations in reflected radiation sensed by an Airborne Thematic Mapper. The definition of LAI used here is the vertical sum of projected leaf surface area of all plants (ignoring the leaf angle distribution within the canopy) per unit of ground area.

Background

The interaction of radiation with the canopy is strongly dependent on wavelength. In the visible region of the electro-magnetic spectrum, radiation is absorbed by chlorophyll a and b, associated pigments, carotenoids, and other organic molecules (Hoffer, 1978). The observed reflectance signal should be inversely related to increases in LAI, total chlorophyll content, and biomass. This relationship should also be asymptotic at low levels of LAI. In the near infrared (IR), leaves absorb radiation weakly and either scatter or transmit radiation. Scattering occurs primarily inside the leaves at interfaces between air and cell walls and other microscopic interfaces (Woolley, 1971).

Ratios of spectral measurements such as the ratio of near IR and red radiation, and transforms such as the normalized difference (near IR − red/near IR + red) (Tucker, 1979), thus combine two oppositely varying properties of canopies. The ratio of the near infrared and red combines a positive effect due to scattering, with an inverse variation due to absorption, producing a positive relationship of the ratio with LAI. The ratio also compensates for some of the variation in reflected radiation attributable to differences in topographic position. The ratio, however, does not eliminate the wavelength dependence of atmospheric scattering and absorption.

A large quantity of literature has appeared relating canopy spectral properties to their phytomass and leaf area. Spectral reflectance data measured by hand-held radiometers, aircraft scanners, and satellite data have been investigated singly and in combination for relationships to plant structure for many plant communities. Research on agricultural monocultures (Asrar et al., 1984; Hatfield et al., 1985; Bauer, 1985) has shown that strong positive relationships exist between ratios and transforms of near infrared to red reflectance and total aboveground biomass and LAI. Inverse asymptotic relationships have been observed between red reflectance and LAI that tend to saturate at LAI values of about 2–3. Similar results have been demonstrated for natural communities such as tidal marsh plants (Bartlett and Klemas, 1981), heath (Curran, 1983), wet and dry green biomass of mixed herbaceous species (Tucker et al., 1981; Tucker et al., 1985), and green yield and cover of mesquite and grass associations (McDaniel and Haas, 1982; Musick, 1984). Badhwar and Hall (1985) reported similar results for aspen that were con-

firmed by canopy radiation models. Attempts to relate reflected solar radiation measured by remote sensing to regional variations in the LAI of coniferous forests have not been reported.

Experimental Design and Methods

Many factors influence reflectance of solar radiation from forest stands including canopy variables and community variables. In this study, major sources of variation at the community level, such as canopy closure, have been controlled so that analysis could be isolated to regional variations in LAI.

The structural properties of canopies that determine the interception and reflection of solar radiation are, in order of importance (Jarvis and Leverenz, 1984): a) LAI, b) vertical distribution of foliage, c) distribution of leaf inclination angles, d) leaf reflectance, transmittance, and scattering properties, e) the grouping or clumpiness of the foliage, and f) the distribution of leaf azimuthal angles. The hypothesis in this study is that variations in LAI between forest ecosystems at the regional level are related to variations observed in spectral reflectance. Factors b)–f), while potentially important within the canopy, were not systematically studied along this regional transect.

Most of the conifers in the western United States are in mountainous terrain. The effect exerted by topographic variations on remote sensing of forests in mountainous areas consist of differences in the atmospheric path length due to elevation, and differences in solar incidence angles due to slope and aspect. Differences in air mass properties caused by orographic effects and geographic proximity to the Pacific Ocean result in varying atmospheric conditions. Particulates (aerosols) and molecular gases in the atmosphere differentially scatter and absorb incoming solar radiation. The particulate and molecular gas content of the atmosphere varies due to changes in air mass and elevation (Potter, 1969). To account for these differences, spectral measurements of each stand and other targets in their vicinity were obtained with a helicopter-mounted radiometer hovering overhead at nearly the same time as the overpass by the aircraft carrying the Airborne Thematic Mapper. This measurement set permitted the calculation of corrections for the effect of the atmosphere for each stand.

Study sites

A transect of forest stands originally established by Gholz (1982) was analyzed for this study. The transect offers virtually the worldwide range of LAI within a relatively short geographic distance. Two mountain ranges lie perpendicular to the flow of moist air masses off the Pacific Ocean, creating an environmental gradient across which LAI varies from greater than 15 to less than 1 proceeding from west to east (Waring and Franklin, 1979). The location of the transect relative to the seven conifer zones of Oregon is shown in Fig. 1. Eighteen stands were located for this study; six correspond to sites measured by Gholz. Each stand was judged for homogeneity and planar topography over an area of at least 7 ha. The elevation differences between the sites are shown in Fig. 2.

Vegetation zone 1 consists of forests of the western coast range dominated by sitka spruce (*Picea sitchensis*) and western hemlock (*Tsuga heterophylla*) with

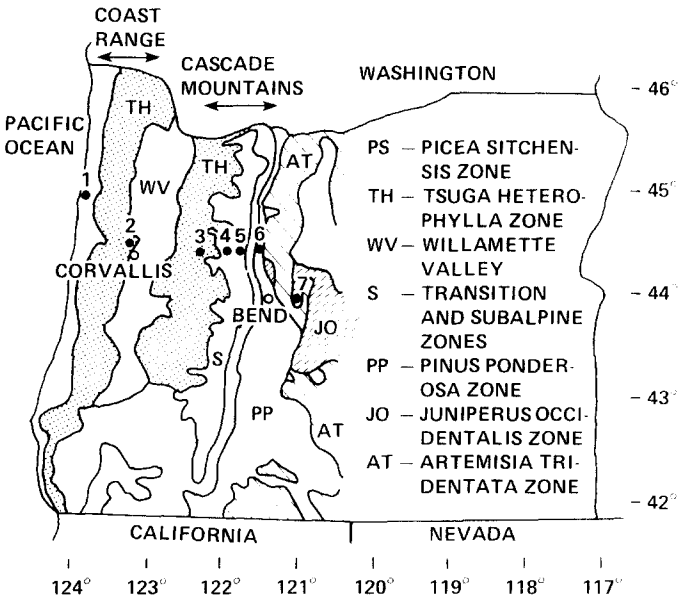

FIGURE 1. Location of the seven vegetation zones and the areas sampled in Oregon (after Gholz, 1982).

very high leaf area. Zone 2 occurs on the inland side of the coast range where the drier, cooler climate produces stands of lower leaf area codominated by western hemlock, Douglas fir (*Pseudotsuga menzeisii*), and grand fir (*Abies grandis*). Five stands were selected in the Cascade Range. Two uniform stands of second-growth Douglas fir were located in the low elevation west Cascades in zone 3. Zone 4 is a transition zone dominated by mixed species forests of Pacific silver fir

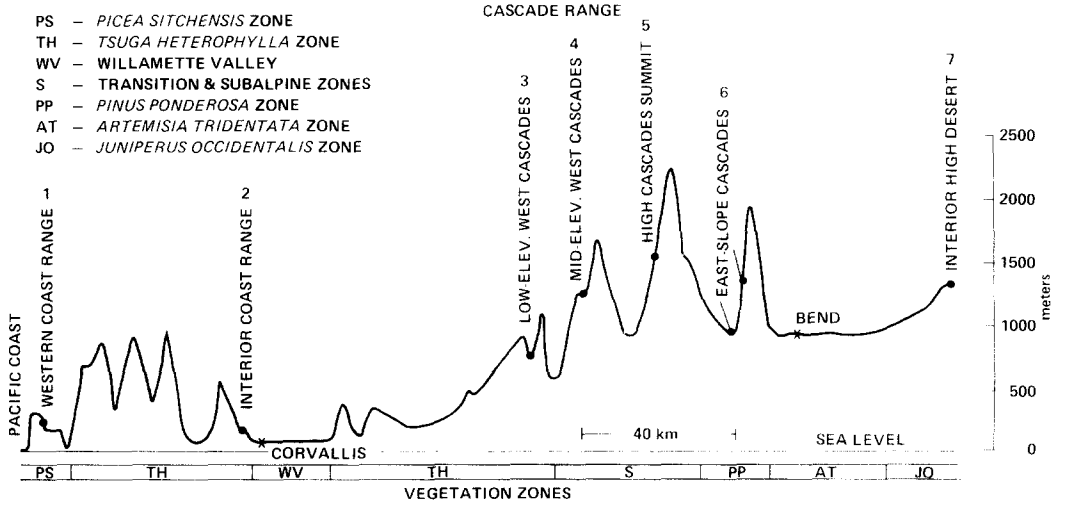

FIGURE 2. Elevational cross section, vegetation zones, and location of sampling points across the transect in west-central Oregon.

(*Abies amabilis*), noble fir (*Abies procera*), and Douglas fir with high leaf area development. At the highest elevations in the transect, subalpine forests of mountain hemlock (*Tsuga mertensiana*), lodgepole pine (*Pinus contorta*), and subalpine fir (*Abies lasiocarpa*) were sampled.

In the rain shadow of the Cascade Mountains, much drier and continentally influenced climates produce lower leaf area development. Zone 6 is dominated by stands of ponderosa pine (*Pinus ponderosa*) in relatively pure stands; three stands were selected here. Two additional stands of white fir (*Abies concolor*), western larch (*Larix occidentals*), and Douglas fir were sampled in this zone at higher elevations on the northwest flank of a cinder cone. Zone 7 is located in the interior high desert of Oregon, characterized by large mesas, continenal climates, low rainfall, and simple communities of low stature. Two open stands dominated by western juniper (*Juniperus occidentalis*) and big sage (*Artemesia tridentata*) with low leaf area index were established here.

Field data

The 18 stands were delineated on optical bar panoramic aerial photography and field checked for condition and relative homogeneity. Four plots were located in each stand. Each plot was planimetrically square and approximately 0.1 ha (30×30 m) in size. The plot locations were diagonally opposed about the centroid of the stand at random distances in the four quadrants.

A complete enumeration of all trees with a bole diameter greater than 5 cm was made for all plots. The species type, its bole diameter at breast height (dbh) (basal circumference for western juniper), crown-to-stem height ratio, crown condition (live/dead), and relative crown position were recorded. An evenly distributed subsample of trees were selected by species and dbh class for detailed measurement. Sapwood thickness, bark thickness, 10-year radial growth increment, and tree age were measured from increment cores taken at breast height. Tree height was also recorded for the subsample. Understory vegetation consisted of various small trees less than 5 cm dbh, shrubs, herbs, and ferns. The understory vegetation was sampled from four 1-m square plots placed equidistance along one diagonal of each plot.

The foliage biomass (dry weight) of each overstory tree was calculated from allometric relations. These allometric relations were developed during the Coniferous Forest Biome studies of the International Biological Program for coniferous forests in western Oregon (Gholz et al., 1979). The allometric relations are usually in logarithmic form, $\ln(y) = a + b \ln(x)$, where y is some variable of interest, such as foliage dry weight, and x is an easily measured variable, such as diameter at breast height or sapwood basal area. Coefficients of determination for these relations are very high, ranging from 0.84 to 0.99. Diameter at breast height was used to calculate foliage properties for all of the tree species. Sapwood basal area is the water-conducting area of tree boles and has been shown to be strongly related to foliage properties such as LAI (Waring et al., 1982). Sapwood basal area equations were used to calculate foliage biomass for Douglas fir and ponderosa pine. These estimates were compared to the dbh-based estimates for the two species.

Foliage biomass was converted to leaf surface area for each plant using surface area to dry weight ratios (Gholz et al., 1979). A value of approximately 2.3 was used to convert from leaf surface area to projected leaf area index for conifers. Leaf area index was calculated for each plot by summing the leaf area index for all plants and dividing by the area of the fixed plot. The average overstory and understory LAI for the four plots at each stand was calculated to derive the total LAI for each forest stand.

Remote sensing data

Multispectral scanner imagery and near-surface multispectral calibration measurements were obtained for each stand using instruments on NASA's ER-2 high altitude aircraft and a commercial Bell-47 helicopter, respectively. The imagery was acquired using the Daedalus Airborne Thematic Mapper (ATM). The ATM simulates the radiometric and spectral characteristics of the Landsat-4 and Landsat-5 Thematic Mapper. At a flight altitude of 19,800 m, the spatial resolution of the ATM data was approximately 24 m. At this altitude the sensor was above most of the earth's atmosphere. The data were taken near solar noon on 15 August 1983. Data acquired from north–south trending flightlines were analyzed.

The near surface measurements were obtained with a Barnes 12-1000A Modular Multiband Radiometer (MMR) with bands simulating the Thematic Mapper bands. The helicopter on which the Barnes MMR was mounted hovered at about 100 m above the canopy. The radiometer has a 15° field of view, producing a 25-m-diameter ground sample. Five independent radiance measurements were recorded over each target. The data were taken for vegetation Zones 3–7 on 15 August and Zones 1 and 2 on 16 August 1983. All data were obtained within 3 hr before and after solar noon. For each vegetation zone, targets measured in addition to the stands included a highly reflective surface (such as a dry grass field, stubble field, or recent clear cut), a highly absorbing surface (such as asphalt runways or a deep body of water), and several targets of intermediate reflectance including various aged forest stands. The number of common targets at each zone ranged from three to nine. An inadequate sample was obtained for several zones because sites observed by the helicopter instrument were narrowly missed by the ATM data path. Weather conditions were excellent with visibility exceeding 40 km on 15 August and 30 km on 16 August.

Reflectance calibration measurements were obtained prior to and following each geographically grouped series of ground measurements. The calibrations consisted of radiance measurements of a 2-ft square barium sulfate reference panel lying horizontal and fully exposed to direct solar illumination. The radiometer was calibrated in the laboratory to a light source traceable to the National Bureau of Standards. Voltages measured by the radiometer were converted to radiance ($mW/cm^2\ \mu m\ sr$) using the calibrations calculated in the laboratory.

The locations of the 18 stands were delineated on the ATM data using an interactive display. Mean digital numbers for the stands in each band were converted to radiance ($mW/cm^2\ \mu m\ sr$) using calibration coefficients published in the flight summary report.

The effects of additive path radiance and transmittance of the atmosphere on

sensor-measured radiance were evaluated by regression analysis of the corresponding radiance measured by the the ATM and the Barnes MMR for each vegetation zone. A simple least-squares linear correlation $y = a + bx$ was used to determine the coefficients a and b, where x is the Barnes radiance and y is the Daedalus radiance (Dana, 1978). The intercept a corresponds to the additive path radiance of a black target. The slope of the regression line b is approximately related to the atmospheric transmittance. The relationship is complicated by atmospheric absorption of reflected radiation and multiple scattering (Fraser and Kaufmann, 1985). The cosine of the solar zenith angles for the ATM and MMR data was calculated, and the MMR data were normalized to the same solar zenith angle present at the time of the ATM overpass. Effects of the atmosphere were corrected using the regression technique for each band at each of the seven geographic zones.

The variation of the terrain between stands (slope and aspect) produced differences in the solar incidence angle. This effect was corrected for each ATM band using the following formula after Smith et al. (1980) which calculates the cosine of the solar zenith angle relative to the local terrain angle:

$$\cos i = \cos\theta_s \cos\theta_n + \sin\theta_s \sin\theta_n \cos(\phi_s - \phi_n),$$

where i is the effective incidence angle, θ_s is the solar zenith angle, θ_n is the slope of the terrain, and ϕ_s and ϕ_n are the azimuth angles of the sun and terrain, respectively. This cosine calculation was used to correct each band after the atmospheric corrections were performed.

Results and Discussion

Field data

The structural and foliage biomass properties of each stand are listed in Table 1. Each number is the average value of the four plots per stand. The regional variation in LAI was from 0.6 to 16.1. The transect across the Oregon forests produced a well-distributed range in LAI. No single tree species occurred at all sites, although Douglas fir was present in mixed communities across the greatest range of environmental conditions and was dominant or codominant in Zones 2, 3, and 6. Fourteen species were codominant across the transect. The highest LAI occurred at Zone 1, the coastal site of western hemlock and sitka spruce, and in Zone 4, in the midelevation west Cascades (Fig. 3). The lowest LAI was obtained in stands dominated by ponderosa pine and western juniper, in the east slope of the Cascades and in the interior high desert, respectively.

Understory LAI had a large variation, ranging from 3.15 and 3.19 in the coastal and low-elevation Cascade sites, to virtually no understory vegetation (0.02–0.05) in the interior stands. The understory provided a significant contribution (10–37%) of total LAI for all mesic environment stands, i.e., those west of the Cascade crest. While there was a greater than 20-fold range in LAI, there was only a fivefold variation in foliage biomass, indicative of the differences in leaf area to dry weight ratios for these species. The coefficient of variation of the LAI of the four plots in each stand ranged from 0.07 to 0.63, indicating the variability of LAI

TABLE 1 Biophysical Characteristics of the Forest Stands

Vegetation Zone	Dominant Tree Species	Stand	Over story LAI	Underst. LAI	Total LAI	% LAI of Under story	Foliage Biomass (kg/ha)	Average DBH (cm)	Average Basal Area (m^2/ha)	Average Stem Density (trees/ha)	Average Stand Height (m)	Coefficient of Variation (LAI%)	Raw Near IR/Red	atm Corr. Near IR/Red
Western coast range,	Western hemlock	9	15.4	0.71	16.1	5	22,890	34.7	114.6	1115	44.2	9.01	3.379	8.1
	sitka spruce	11	11.1	2.31	13.4	17	16,690	58.6	99.1	283	46.2	19.63	3.036	9.102
Zone 1	Sitka spruce	10	5.7	3.15	8.8	37	9770	55.6	120.5	410	48.8	16.02	2.786	8.054
Interior coast range,	Douglas fir	8	5.0	1.31	6.3	20	9980	50.5	62.5	220	43.9	62.86	2.634	6.104
Zone 2	Grand fir, Western hemlock	18	4.0	0.87	4.8	18	8650	45.5	44.2	180	37.8	32.92	2.824	5.958
Low-elev. west Cascades, Zone 3	Douglas fir	13	6.5	3.19	9.7	33	12,160	34.0	59.7	505	39.1	19.69	2.828	7.173
		17	6.7	2.23	8.9	27	13,590	35.2	62.1	493	37.9	8.54	2.443	6.186
Mid-elev. west Cascades, Zone 4	Western hemlock, Douglas fir Pacific silver fir, noble fir	12	10.9	0.55	11.4	5	19,860	24.0	95.1	1390	29.1	15.53	3.450	9.260
High Cascades summit, Zone 5	Lodgepole pine	6	5.2	1.73	6.9	26	10,900	13.2	52.6	2620	8.8		2.383	5.065
	Subalpine fir	7	3.9	1.28	5.1	25	10,410	12.7	44.6	2668	8.8	34.71	1.927	3.750
	Mountain hemlock	16	4.5	1.05	5.5	10	13,720	23.0	59.4	1045	18.2	7.45	2.080	4.373
East slope Cascades, Zone 6	White fir	5	5.1	0.02	5.2	0.4	13,210	12.5	46.9	2370	24.2	14.19	1.396	4.975
	Douglas fir, white fir	4	5.4	0.02	5.4	0.4	12,350	18.7	56.5	1525	19.7	19.81	2.722	5.570
	Ponderosa pine, Douglas fir	3	3.1	0.04	3.2	1.2	9170	30.1	33.0	373	24.4	30.31	1.558	1.919
	Ponderosa pine	14	3.1	0.20	3.3	6	9520	15.4	34.9	1085	28.0	33.33	1.870	2.626
		15	2.8	0.15	3.0	5	8280	114	35.4	1761	20.6	34.67	1.759	2.375
Interior high desert, Zone 7	Western juniper	1	0.6	0.05	0.6	8	4260	77.4[a]	22.4	265	12.4	13.33	0.8066	0.773
		2	0.6	0.05	0.7	7	4790	124.2[a]	26.0	154	17.6	32.86	0.8174	0.787

[a] Basal circumference for Western juniper.

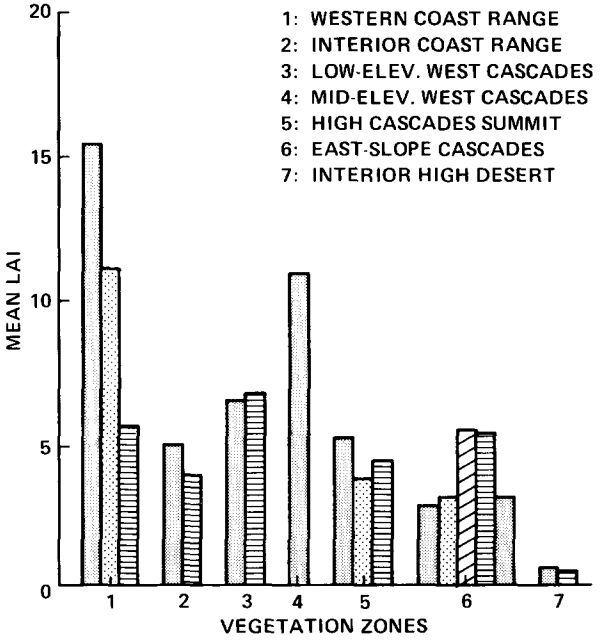

FIGURE 3. Bar chart showing the distribution of LAI for the 18 stands.

at the stand level. All of the stands were relatively mature, well stocked, and undisturbed, and conformed to the inverse relationship of stem density to average dbh (DeAngelis et al., 1981). The youngest stands were regeneration stands of lodgepole pine (Stands 6 and 7), with the lowest average basal area and dbh, and highest stem densities.

Marshall and Waring (1986) compared the differences between dbh and sapwood basal area techniques for determining the LAI of old-growth Douglas fir and found that dbh overestimated LAI. A comparison of LAI estimated by dbh and by sapwood basal area for individual trees from our plots for Douglas fir and for ponderosa pine is shown in Figs. 4 and 5, respectively. For trees smaller than 50 cm dbh (roughly equivalent to a leaf surface area of 350 m^2), the two techniques provided similar results. For trees with a dbh exceeding 50 cm, dbh-based measurements overestimated LAI relative to sapwood for both species. The critical concern was whether the overestimates of individual trees had a large effect at the plot and stand level. The effect was small in the stands investigated because the tree size distribution tended to be dominated by smaller trees. Most of the trees in the stands analyzed were second growth, with a dbh of less than 50 cm. The smaller trees were well estimated by the dbh equations, and contributed the greatest proportion to the LAI of most of the stands.

Remote sensing data

The relationship between near IR radiance corrected for atmospheric and topographic effects and LAI for each stand is shown in Fig. 6. The relationship was virtually flat with little correlation between LAI and near IR radiance. The coefficient of determination was 0.04. The

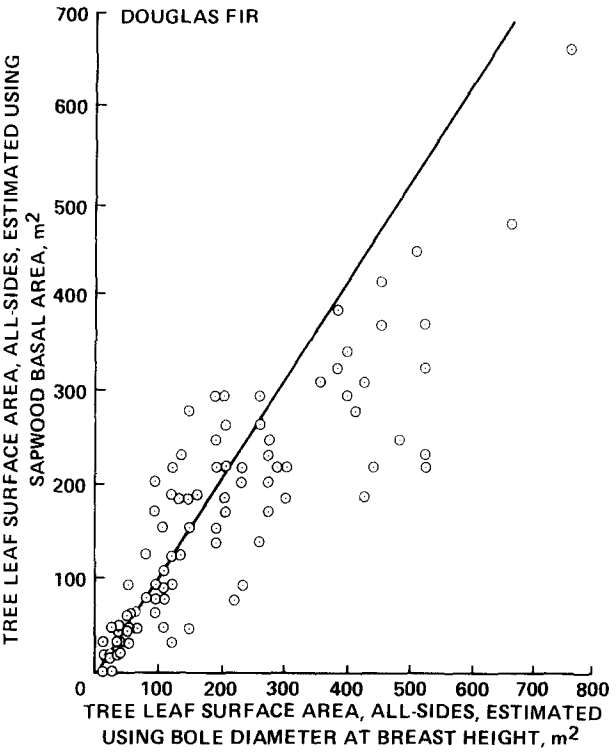

FIGURE 4. Relationship of tree leaf surface area estimated by sapwood basal area and bole diameter at breast height for Douglas fir.

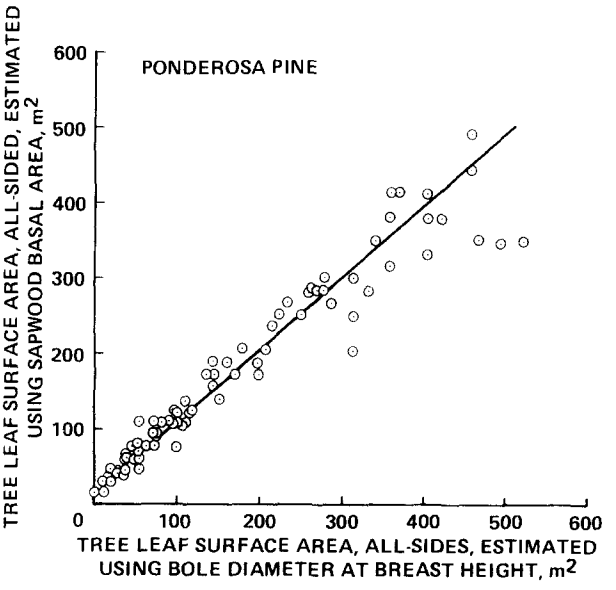

FIGURE 5. Relationship of tree leaf surface area estimated by sapwood basal area and bole diameter at breast height for ponderosa pine.

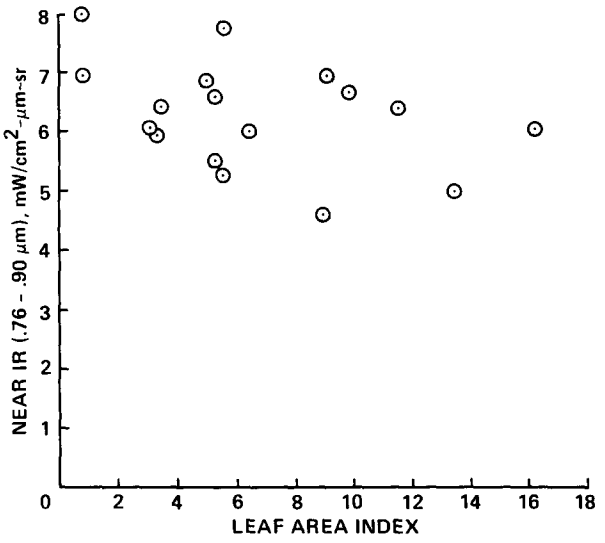

FIGURE 6. Relationship between near IR radiance corrected for atmospheric and topographic effects and the LAI of the forest stands.

range of radiances for the forest stands in the near IR was relatively narrow, varying from 4.5 to 8.2 mW/cm^2 μm sr. This twofold range in near IR radiance compares to a greater than 20-fold range in LAI. The relationship between LAI and near IR radiance was unexpectedly flat despite the inclusion of 14 different species across the transect and a very wide range in structure and architecture of the stands. There were some spectral differences between the conifer communities, but it is unlikely that the flat response in the near IR was due to differences in the spectral reflectance of the needles themselves.

A possible explanation for the flat response in the near IR is the spatial organization and characteristic shape of conifer needles. Norman and Jarvis (1975) showed that the clumpiness of the needles in sitka spruce was important in predicting the penetration of radiation directly into the canopy. The rounded cross section and small lateral dimension of needles contribute to their ability to scatter radiation. Also, the architecture of natural forest stands result in canopies being positioned at different heights. The stand may appear to have a closed canopy from nadir; however, there are many direct openings to the sky at off-nadir angles. This permits significant amounts of radiation to directly penetrate the canopy without encountering needles. Radiation would be subject to absorption by both the needles and the bark of the bole and branches. These properties of the canopy contribute together to enhance light harvesting by the conifer canopies in a manner similar to the principles used to design black body radiators.

The relationship of the atmospheric and topographically corrected red radiance and LAI, shown in Fig. 7, was consistent with the expected inverse and asymptotic behavior due to chlorophyll absorption. The linear regression explained 55% of the variance. A log-linear equation of the form $y = ax^b$, where y is the near IR/red

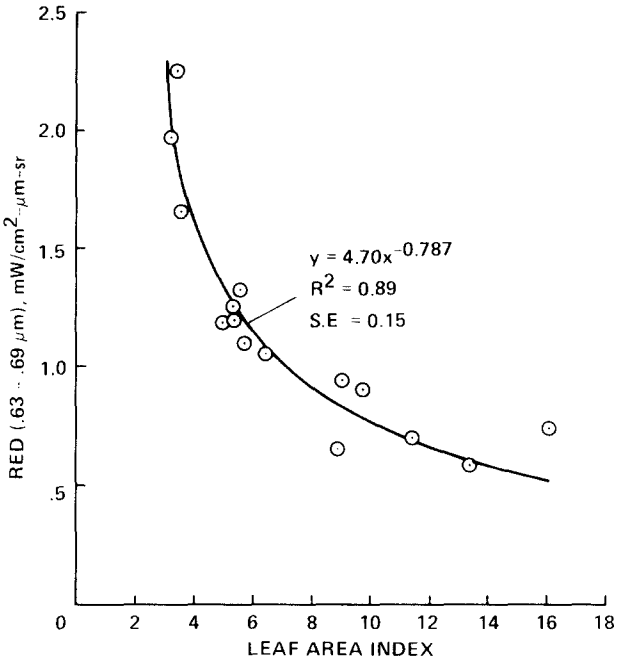

FIGURE 7. Relationship between red radiance corrected for atmospheric and topographic effects and the LAI of the forest stands.

ratio, x is LAI, and a and b are the coefficients, explained 89% of the variance. The data shown do not include values for western juniper, which had very high radiance in the red and reduced the coefficient of determination to 0.36. The range in radiances was from 0.60 to 2.33 mW/cm^2 μm sr. The energy received by the sensor was 4–8 times less than the energy measured in the near IR. Because of the low radiance in the red, additive effects due to path radiance had a stronger influence on red radiation than on near IR radiation. The red radiance decreased relatively slowly with increases in LAI and approached an asymptotic value at an LAI of approximately 8. This result is different from reported crop and grass results, which indicate that the asymptote is reached at an LAI of approximately 3.

The saturation of red radiation at an LAI of about 8 is difficult to explain. Conifer needles are not more or less inherently reflective than other leaves in the red. They do have a thick cuticle which might enhance specular reflection, leading to more penetration of the canopy by red radiation. Perhaps the shape, size, and orientation of needle leaf canopies enhance diffusion of light within the canopy with attendant small differences in the intensity of the scattered radiation in the red. This may also be a factor in explaining why the near IR response is so flat and does not increase with increasing LAI. A great deal more research on conifer canopies is needed to develop a biophysical understanding of these results.

The relationship of the atmospherically corrected near IR/red ratio with the LAI of the plots is shown in Fig. 8. A strong

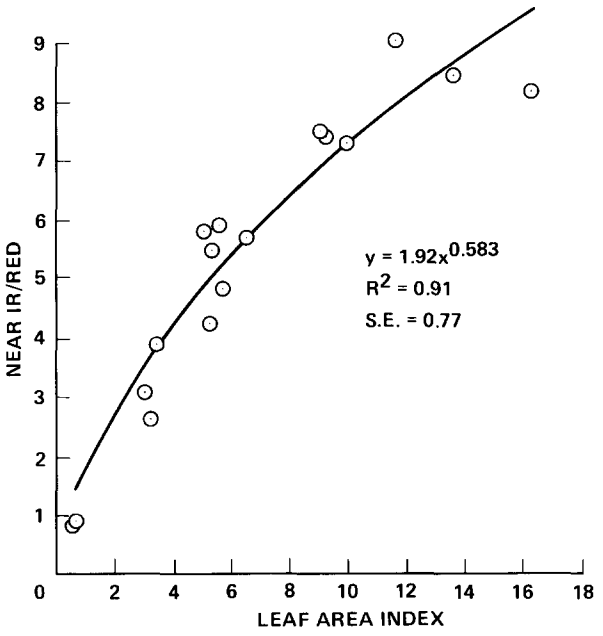

FIGURE 8. Relationship between the atmospherically corrected near IR/red ratio and the LAI of the forest stands.

positive relationship between LAI and the ratio was evident. Since the near IR radiance values did not vary significantly, most of this relationship was due to the inverse behavior of the red radiance. At high levels of LAI, the values of the near IR and red bands tended to vary together, thereby compensating for spectral differences between the stands. A linear regression explained 83% of the variance in the spectral ratio. A log-linear equation explained 91% of the variance. The standard error of the log-linear relation was 0.77, compared to 1.03 for the linear equation. The LAI to near IR/red relationship slowly became asymptotic, reaching a saturation level at about an LAI of ten. This is more than twice as high as the values measured and modeled for crop and grass communities (Sellers, 1985).

To evaluate why the near IR/red ratio produced better results than either band alone, a Monte Carlo simulation of the band ratioing effect was performed (Card, 1986). The band ratio was simulated as the ratio of two normally distributed random variables having equal means and variances. The correlation coefficients between the variables was systematically varied over the range 0–1 to simulate correlated noise between bands. The result of the simulation was expressed in terms of the variance of the ratio. Roughly speaking, the variance of the ratio decreased as the noise in the bands became more correlated. Ratioing tended to decrease the adverse effect of additive noise, the improvement being highest when there was significant noise correlation between the bands.

A scatter plot of the stands for the near IR and red bands is shown in Fig. 9. Also shown on this figure are isolines of equal ratios of the near IR and red bands. Spectral differences between the stands are

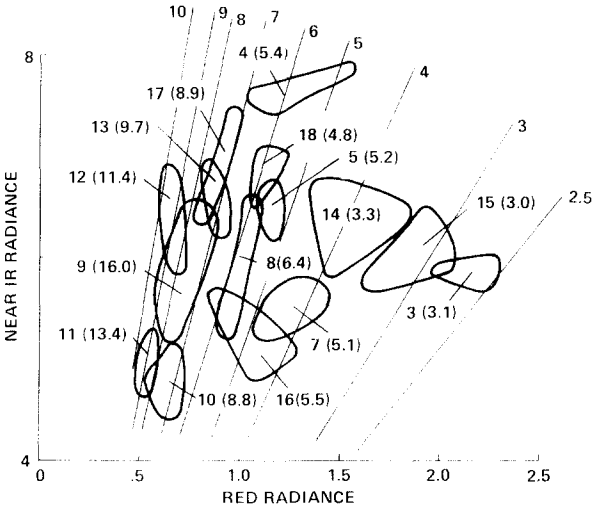

FIGURE 9. Ellipse plot of each stand (excluding western juniper) for red and near IR radiance. Stand number and LAI (in parenthesis) are indicated. Isolines indicate the near IR/red ratio values. Areas of the ellipse indicate plot values within the stand.

evident. Average stand LAI values occur along the same isoline, indicating that the near IR/red ratio compensated for spectral differences between the stands. Differences at low LAI in the red were due to variations in background reflectance under more open canopies.

A comparison of the relationships between the uncorrected and atmospherically corrected ratios of the near IR and red bands and LAI is given in Fig. 10. Each point is the average of the four plots per stand; the bars indicate the variation in LAI for the stand. For the linear regression, the coefficient of determination improved from 0.76 for the uncorrected data to 0.83 for the atmospherically corrected data. This difference was not significant at the 0.05 level. Of interest, however, was the strong suppression of the ratio values when the atmospheric effects were not removed from the data. Comparing the regression equations, the slope of the relation increased more than three times from 0.167 to 0.532 for the atmospherically corrected data. For a given change in LAI, there was a threefold smaller change in the raw ratio than in the atmospherically corrected ratio. The standard error of the regression equation increased from 0.38 to 1.03 after atmospheric corrections were applied.

A method to compare the sensitivities of two regression relationships that corrects for different residual errors was given by Mandel (1964). He defined a relative sensitivity (RS) for two variables, M and N, each a function of an independent variable X (LAI in this case), as

$$\mathrm{RS} = B(M)/B(N)/\mathrm{SE}(M)/\mathrm{SE}(N),$$

where $B(M)$ and $B(N)$ are the slopes of the linear regression lines for the variables M and N vs. X, respectively, and $\mathrm{SE}(M)$ and $\mathrm{SE}(N)$ are the corresponding residual standard errors. A value of RS exceeding 1 indicates that the variable M is more sensitive to differences in the independent variable X than is N. The

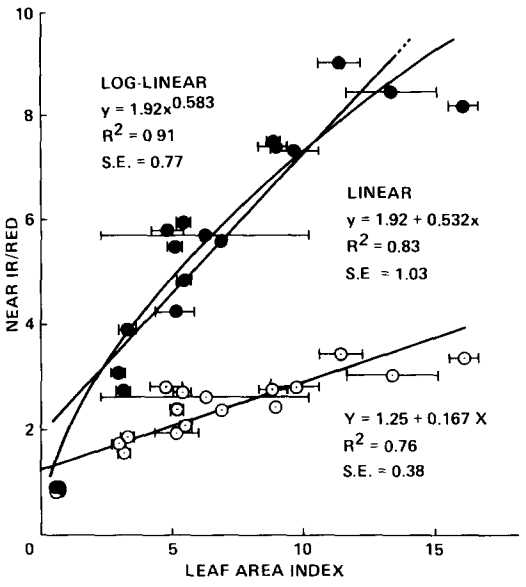

FIGURE 10. Relationship between uncorrected (light circles) and atmospherically corrected (dark circles) near IR/red ratios and the LAI of the forest stands.

value of RS for these data was 1.18, indicating that the atmospherically corrected near IR/red ratio (M) was more sensitive to differences in LAI than was the uncorrected near IR/red ratio (N).

The dynamic range of the near IR/red ratio for the atmospherically corrected data increased from 0.8–3.6 to 0.8–9.0 (Table 1). The atmosphere provided approximately 60% of the signal over conifer canopies in the red, and 20% of the near IR signal. The larger proportion of additive radiance in the denominator of the IR/red ratio caused the reduction of the dynamic range of the uncorrected ratio. The effect of the atmosphere was closely related to elevational differences. At higher elevations with reduced atmospheric pressure, Rayleigh scattering decreased, thereby reducing the path radiance (Spanner et al., 1984).

The sensitivity of other spectral bands and band combinations to LAI were analyzed. The results shown in Table 2 are for overstory LAI only, but are similar to the results for total LAI. The linear correlation of LAI to any one band was low in all cases; the weakest relationship was in the near IR. A consistent inverse correlation was observed for bands in the blue (0.45–0.52 μm), green (0.52–0.60

TABLE 2 Coefficients of Determination for Linear Regression Between LAI and Various Combinations of Bands for the Uncorrected Data

Spectral Variable	Coefficient of Determination
Blue (0.45–0.52 μm)	0.28
Green (0.52–0.60 μm)	0.29
Red (0.63–0.69 μm)	0.35
Near IR (0.76–0.90 μm)	0.26
Shortwave IR_1 (1.55–1.75 μm)	0.38
Shortwave IR_2 (2.08–2.35 μm)	0.37
Near IR/red	0.71
Near IR/shortwave IR_1	0.65
Near IR/shortwave IR_2	0.70
Normalized difference (near IR, red)	0.55
Transformed normalized difference (near IR, red)	0.51
Brightness	0.33
Greenness	0.63
Wetness	0.56

TABLE 3 Coefficients of Determination for Linear Regression Between Forest Parameters

	LAI	Stem Density	Foilage Biomass	Estimated Volume	Basal Area
LAI	1.00	0.20	0.76	0.61	0.72
Stem density		1.00	0.07	0.05	0.00
Foilage biomass			1.00	0.35	0.58
Estimated volume				1.00	0.86
Basal area					1.00

TABLE 4 Coefficients of Determination for Linear Regression Between Forest Parameters and Atmospherically Corrected Spectral Data

	Spectral Variable		
Forest Parameter	Red	Near IR	Near IR/Red
Foliage biomass	0.31	0.04	0.54
Estimated volume	0.21	0.22	0.51
Stem density	0.07	0.01	0.03
Basal area	0.27	0.20	0.59

μm), and in the shortwave infrared (1.55–1.75 and 2.08–2.35 μm). Among the band ratios tested, the near IR/red ratio provided the strongest relationship to LAI, followed closely by ratios of the near IR and shortwave IR bands. The latter two ratios combine near infrared radiance with absorption due to water in the shortwave IR (Gausman and Allen, 1971). The normalized difference of the near IR and red, its transform, and the tasseled cap transformations of brightness, greenness, and wetness (Crist and Cicone, 1984) were all less correlated to LAI than was the near IR/red ratio.

The question remains whether the near IR/red ratio can be explained by some other forest variable that is highly correlated to LAI. The correlation between stand variables is presented in Table 3. LAI was not correlated with stem density, but moderate correlations occurred with estimated volume, stand basal area, and foliage biomass. The relationship to basal area was a consequence of the allometric relations used to calculate LAI from basal diameter. Estimated stand volume is based on average height times basal area. Because height varied more slowly than basal area across the stands, the stronger influence of basal area on volume accounted for the correlation with LAI. Each of the other stand variables were compared with the red and near IR bands and its ratio (Table 4). Stem density had no relationship to any radiance variable. None of the stand variables explained near IR radiance. Estimated volume, basal area, and foliage biomass were correlated with the red band and the near IR/red ratio with correlation coefficients ranging from 0.21 to 0.59. None of the stand variables explained the IR/red ratio as well as LAI did.

Conclusions

The results provide evidence that the LAI of temperate coniferous forests across a regional gradient is related to the ratio of the near infrared and red spectral bands measured by the Airborne Thematic Mapper. The LAI of mostly closed canopy

coniferous forests explained most of the variation in the near IR/red ratio. The regional transect included 14 different species of conifers, including one species, Douglas fir, that was codominant across a wide range of environmental conditions. The LAI to near IR/red relationship slowly become asymptotic, reaching a saturation level at an LAI of 10, more than twice as high as values reported for crop and grass communities. The relationship of LAI to the red band was inversely asymptotic, reaching saturation at an LAI of approximately eight. An advantage of using the near IR/red ratio instead of the red band for estimation of LAI is that residual terrain effects are removed by the ratio.

Radiance measured in the near infrared for the large range of LAI was fairly constant across the transect. Most earlier studies involving broadleaf plants indicated that a strong positive relationship existed between LAI and near IR radiance. The flat response to the LAI of conifers in the near IR probably contributes to the difficulty researchers have found in attempting to spectrally discriminate different classes of conifer communities. The near IR/red ratio appeared to compensate for small differences in the spectral quality of the various communities across the transect. Removal of the atmospheric effects produced a threefold increase in the slope of the LAI-near IR/red regression line. The sensitivity of the ratio to atmospheric effects points out the importance of atmospheric models to systematically and accurately remove these effects. The near IR/red ratio without correction for atmospheric effects, however, achieved nearly the same coefficient of determination with LAI as the atmospherically corrected data.

The generality of these relationships cannot be assumed until further research in other forest communities is accomplished. Most of the stands selected for this study had nearly closed canopies and were mature forests. Research involving the remote sensing of forests with open stands and different understory conditions, of forests with a mixed canopy of conifer and broadleaf trees or plants, of plantations with very even structural properties, and of stands across a variety of successional ages is required to assess the generality of these results. Management of forest resources is usually confined to smaller geographic regions than used in this study, usually within one vegetation zone. While these results indicate that most of the variation of the LAI of conifer forests in the seven vegetation zones was explained by the near IR/red ratio, application of the regional level results to within-vegetation zone LAI estimation is not warranted.

The heterogeneity observed within forest stands and the variation in spectral properties at the local level were not solely explained by variations in LAI. These results, however, support the potential to use remotely sensed information to describe differences in LAI for regional ecological studies. The results can be used for this transect to extrapolate from LAI to above ground net primary production shown by Gholz (1982), using the synoptic measurements provided by remote sensing instruments.

The authors gratefully acknowledge the advice and insights provided by Dr. Henry Gholz of the University of Florida, to the important role of Ms. Madeline Hall of the Oregon State University in obtaining the helicopter measurements, and the ad-

vice and help provided by Mr. Don Card, Mr. Robert Wrigley, and Mr. William Acevedo of NASA Ames for various aspects of the analysis. The work was supported by research grants from NASA's Global Biology Program, Grant No. 199-30-32-01, and NASA's Terrestrial Ecosystems Program, Grant No. 677-21-31, as well as Ames Joint Research Interchange NCA2-OR475-301 with the University of Montana.

References

Asrar, G., Fuchs, M., Kanemasu, E. T., and Hatfield, J. L. (1984), Estimating absorbed photosynthetic radiation and leaf area index from spectral reflectance in wheat, *Agron. J.* 76:300–306.

Badhwar, G. D., and Hall, F. G. (1985), Mapping of vegetation, leaf area index, and primary productivity in the Boundary Water Canoe Area using Landsat data, in *Proc. of Int. Conf. on Man's Role in Changing the Global Environment*, Venice, Italy, 21–26 October 1985.

Bartlett, D. S., and Klemas, V. (1981), In situ spectral reflectance studies of tidal wetland grasses, *Photgramm. Eng. Remote Sens.* 47:1695–1703.

Bauer, M. E. (1985), Spectral inputs to crop identification and condition assessment, *Proc. IEEE* 73(6):1071–1085.

Card, D. H. (1986), personal communication, NASA Ames Research Center.

Crist, E. P., and Cicone, R. C. (1984), A physically-based transformation of Thematic Mapper data—the TM tasseled cap, *IEEE Trans. Geosci. Remote Sens.* GE-22(3):256–263.

Curran, P. J. (1983), Estimating green leaf area index from multispectral aerial photography, *Photogramm. Eng. Remote Sens.* 49(12):1709–1720.

Dana, R. W. (1978), Using airborne radiometry to determine atmospheric effects in Landsat data, in *Proc. Am. Soc. of Photogrammetry*, Fall meeting, Albuquerque, NM, pp. 117–128.

DeAngelis, D. L., Gardner, R. H., and Shugart H. H. (1981), Productivity of forest ecosystems studied during the IBP: the woodlands data set, in *Dynamic Properties of Forest Ecosystems* (D.E. Reichle, Ed.), Cambridge Univ. Press, Cambridge, Chap. 10, pp. 567–672.

Fraser, R. S., and Kaufmann, Y. J. (1985), The relative importance of aerosol scattering and absorption in remote sensing, *IEEE Trans. Geosci. Remote Sens.* GE-22(6):625–633.

Gausman, H. W., and Allen, W. A. (1973), Optical parameters of leaves of 30 plant species, *Plant Physiol.* 52:57–62.

Gholz, H. L., (1982), Environmental limits on aboveground net primary production, leaf area, and biomass in vegetation zones of the Pacific Northwest, *Ecology* 63(2):469–481.

Gholz, H. L., Grier, C. C., Campbell, A. G., and Brown, A. T. (1979), Equations for estimating biomass and leaf area of plants in the Pacific Northwest, Res. Paper 41, Forest Research Lab, Oregon State University, Corvallis, OR, 39 pp.

Grier, C. C., and Running, S. W. (1977), Leaf area of mature Northwestern coniferous forests: relation to site water balance, *Ecology* 58(4):893–899.

Hatfield, J. T., Kanemasu, E. T., Asrar, G., Jackson, R. J., Pinter, P. J., Reginato, R. J., and Idso, S. B. (1985), Leaf area estimates from spectral reflectance measurements over various planting dates of wheat, *Int. J. Remote Sens.* 6(1):167–175.

Hoffer, R. M. (1978), Biological and physical considerations in applying computer-aided analysis techniques to remote sensing data, in *Remote Sensing: The Quantitative Approach* (Swain and Davis, Eds.), McGraw-

Hill International, New York, Chap. 5, 396 pp.

Jarvis, P. G., and Leverenz, J. W. (1984), Productivity of temperate, deciduous and evergreen forests, in *Physiological Plant Ecology IV* (O. L. Lange, P. S. Nobel, C. B. Osmond, and H. Zeigler, Eds.), Springer-Verlag, New York, Chap. 8, pp. 233–280.

Mandel, J. (1964), *The Statistical Analysis of Data*, Wiley-Interscience, New York, 410 pp.

Marshall, J. D., and Waring, R. H. (1986), Comparison of methods of estimating leaf area index in old growth Douglas fir, *Ecology* 67(4):975–979.

McDaniel, K. C., and Haas, R. H. (1982), Assessing mesquite-grass vegetation condition from Landsat, *Photogramm. Eng. Remote Sens.* 48(3):441–450.

Musick, H. B. (1984), Assessment of Landsat MSS spectral indexes for monitoring arid grassland, *IEEE Trans. Geosci. Remote Sens.* GE-22:512–519.

Norman, J. M., and Jarvis, P. G. (1975), Photosynthesis in Sitka spruce, V: Radiation penetration theory and a test case, *J. Appl. Ecol.* 12(3):839–878.

Potter, J. F. (1969), Scattering and absorption in the earths atmosphere, in *Proc. Sixth Int. Symp. on Remote Sensing of Environment*, pp. 415–429.

Rambler, M. B., Ed. (1983), Global Biology Research Program, NASA TM 85629.

Running, S. W. (1984), Microclimate control of forest productivity: Analysis by computer simulation of annual photosynthesis/transpiration balance in different environments, *Ag. For. Meteorol.* 32:267–288.

Sellers, P. J. (1985), Canopy reflectance, photosynthesis and transpiration, *Int. J. Remote Sens.* 6(8):1335–1372.

Smith, J. A., Liu, T. L., and Ranson, K. J. (1980), The lambertian assumption and Landsat data, *Photogramm. Eng. Remote Sens.* 46(9):1183–1189.

Spanner, M. A., Peterson, D. L., Hall, M. J., Wrigley, R. C., Card, D. H., and Running, S. W. (1984), Atmospheric effects on the remote sensing estimation of forest leaf area index, *Proc. of 18th Int. Symp. on Remote Sensing Environment*, Paris, France, 1–5 October, pp. 1295–1308.

Tucker, C. J. (1979), Red and photographic infrared linear combinations for monitoring vegetation, *Remote Sens. Environ.* 8(2):127–150.

Tucker, C. J., Holben, B. N., Elgin, J. H., and McMurtrey, J. E. (1981), Remote sensing of total dry-matter accumulation in winter wheat, *Remote Sens. Environ.* 11:171–189.

Tucker, C. J., Vanpraet, C. L., Sharman, M. J., and Van Ittersum, G. (1985), Satellite remote sensing of total herbaceous biomass production in the Senegalese Sahel: 1980–1984, *Remote Sens. Environ.* 17(3):233–249.

Waring, R. H., and Franklin, J. F. (1979), Evergreen coniferous forests of the Pacific Northwest, *Science* 24:131–140.

Waring, R. H., Schroeder, P. E., and Oren, R. (1982), Application of the pipe model theory to predict canopy leaf area, *Can. J. Forest Res.* 12:556–560.

Wittwer, S., Ed. (1983), Land-Related Global Habitability Science Issues, NASA TM 85841.

Woolley, J. T. (1971), Reflectance and transmittance of light by leaves, *Plant Physiol.* 47:656–662.

Received 16 June 1986; revised 19 December 1986.